Chinese Chemical Letters 32 (2021) 685–690

Contents lists available at ScienceDirect

Chinese Chemical Letters

journal homepage: www.elsevier.com/locate/cclet

Communication

The synergistic catalysis on Co nanoparticles and CoN_x sites of aniline-modified ZIF derived Co@NCs for oxidative esterification of HMF

Tao Rui[a], Guo-Ping Lu[a,b,*], Xin Zhao[b], Xun Cao[b], Zhong Chen[b,*]

[a] School of Chemical Engineering, Nanjing University of Science & Technology, Nanjing 210094, China
[b] School of Materials Science & Engineering, Nanyang Technological University, Singapore 639798, Singapore

ARTICLE INFO

Article history:
Received 7 May 2020
Received in revised form 13 June 2020
Accepted 19 June 2020
Available online 22 June 2020

Keywords:
Aniline-modified ZIF
Porous cobalt/nitrogen co-doped carbon
Synergistic catalysis on CoN_x sites and Co nanoparticles
Oxidative esterification
5-Hydroxymethylfurfural

ABSTRACT

An efficient, sustainable and scalable strategy for the synthesis of porous cobalt/nitrogen co-doped carbons (Co@NCs) *via* pyrolysis of aniline-modified ZIFs, has been demonstrated. Aniline can coordinate and absorb on the surface of ZIF (ZIF-CoZn3-PhA), accelerate the precipitation of ZIFs, thus resulting in smaller ZIF particle size. Meanwhile, the aniline on the surface of ZIF-CoZn3-PhA promotes the formation of the protective carbon shell and smaller Co nanoparticles, and increases nitrogen content of the catalyst. Because of these properties of Co@NC-PhA-3, the oxidative esterification of 5-hydroxymethylfurfural can be carried out under ambient conditions. According to our experimental and computational results, a synergistic catalytic effect between CoN_x sites and Co nanoparticles has been established, in which both Co nanoparticles and CoN_x can activate O_2 while Co nanoparticles bind and oxidize HMF. Moreover, the formation and release of active oxygen species in CoN_x sites are reinforced by the electronic interaction between Co nanoparticles and CoN_x.

5-Hydroxymethylfurfural (HMF) derived from carbohydrates or cellulose by dehydration, has been used to bridge the gap between lignocellulosic biomass and some useful chemicals [1–3]. One particularly useful transformation of HMF is its oxidation to 2,5-furandicarboxylicacid (FDCA), one of the top-10 biobased products from biorefinery carbohydrates [4]. FDCA can be used as a monomer for biopolymers that can replace the fossil fuel-derived polyethylene terephthalate (PET) [5]. However, there are difficulties in its direct application in industry due to its low solubility in most solvents and lack of economic methods for its purification [6]. 2,5-Furan dicarboxylicacid dimethyl ester (FDMC) has good solubility in lots of solvents, which can also be used directly to synthesize biopolymers through transesterification reaction [7]. Thus, FDMC is an ideal alternative to FDCA.

This transformation is usually catalyzed by noble metals (Au, Pd) with the help of high pressure or excess bases [8–11]. A few earth-abundant-metal catalysts have also been explored, but high temperature and O_2 pressure are needed, and the selectivity is still poor in some cases [12–14]. To further optimize the reaction conditions, some multi-metal catalysts including Co_xO_y-N@C/Ru@C, PdCoBi@C, AuPd-Fe_3O_4 have been developed [15–17]. More recently, Co,N-codoped carbon materials were foundto be a kind of efficient earth-abundant metal catalysts for the oxidative esterification of HMF under base-free conditions [18–22]. Lin and Zeng suggested that cobalt nanoparticles (Co NPs) activated by the Mott-Schottky effect may be the main catalytic active sites [21,22]. In general, there are two potential catalytic active centers: Co NPs and CoN_x sites in Co@NCs. Eisenberg *et al*. have proposed a new concept of "active doughnut" in which the Co NPs and CoN_x activate O_2 while Co NPs bind and oxidize alcohol [23,24]. Meanwhile, Hu has demonstrated that the electronic interactions between Fe NPs and FeN_4 coordination structure in Fe@NCs favor the adsorption of O_2 [25]. Along this line, we envisage that there is a synergistic catalytic effect between CoN_x sites and Co NPs of Co@NCs for oxidative esterification of HMF, which has not been addressed by any reports so far.

Compared with other materials, zeolitic imidazolate frameworks (ZIFs) serve as ideal precursors for the formation of Co@NCs owing to their low-cost raw materials, mild synthetic conditions, high nitrogen content, and tunable and uniform pore apertures [26]. Zinc as a self-sacrificialtemplate is also introduced to eliminate the aggregation of Co nanoparticles and improve the specific surface areas of Co@NCs during the pyrolysis of ZIFs

* Corresponding author at: School of Materials Science & Engineering,Nanyang Technological University, Singapore 639798, Singapore.
E-mail addresses: glu@njust.edu.cn (G.-P. Lu), ASZChen@ntu.edu.sg (Z. Chen).

https://doi.org/10.1016/j.cclet.2020.06.027
1001-8417/

[27,28]. In addition, the synthesis of ZIFs can be achieved in water, which not only avoids the use of toxic organic solvents, but also helps to save costs of ZIFs [29–33]. There are a few scattered reports mentioning that the reactant concentration and the use of modulators (amino acids, butylamine, CTAB) can affect the particle size and morphology of ZIFs [34–36]. Accordingly, we expect that (1) the use of different amines as the modulators may change both morphology and size of ZIFs in water; (2) amines may adsorb on the surface of ZIFs to form a protective carbon shell after carbonization; (3) some of the Co@NCs derived from amine-modified ZIFs may possess excellent catalytic performance for oxidative esterification of HMF due to their controllable size and morphology or protective carbon shell.

With our interestsin exploring the novel ZIF-derived Co@NCs for organic transformations [19,28,37], we demonstrate an efficient, sustainable and scalable strategy for the synthesis of Co@NCs, in which ZIFs as the precursors, are prepared in water solution using aniline as the modulators. Aniline can significantly affect the size of the ZIFs by adsorbing on the surface of ZIFs and increasing the precipitation of ZIFs. Co@NC-PhA-3 exhibits excellent catalytic performance for oxidative esterification of HMF, which is ascribed to its high BET surface areas, the existence of carbon shell on smaller Co NPs, higher N content and synergistic catalytic effect between its CoN_x sites and Co NPs.

We started the investigation by employing different amines in the synthesis of ZIF-CoZnX-Y (X denotes the mole ratio of Zn/Co, Y the type of amine shown in Fig. S1 in Supporting information) in water. These ZIFs were then pyrolyzed at 900 °C with a heating rate of 5 °C/min for 2 h under pure Ar atmosphere to afford the corresponding Co@NC-Y-X (Fig. S1). Generally, the yields of ZIFs in water are higher than that in MeOH. For example, the yield of ZIF-CoZn3-PhA is higher than 450 mg (2 mmol scale), but the yield of ZIF-CoZn3-M (Table 1) is less than 250 mg even with prolonged reaction time to 24 h.

As shown in Fig. 1, spherical ZIFs were obtained in the presence of amine or in methanol with different particle sizes (Figs. 1a–d and f), while irregular flake and rod ZIFs were yielded in the absence of amine (Fig. 1e). The order of the particle sizes of ZIFs is ZIF-CoZn3-PhA < ZIF-CoZn3-OA < ZIF-CoZn3-*n*BuA < ZIF-CoZn3-BnA < ZIF-CoZn3-M (Fig. 1, Table S1 in Supporting information). Thus, it can be concluded that the type of amines plays a crucial role on the size of ZIFs in water. It is well known that all particle ZIFs are formed by self-assembly of sodalite cages [38]. It is reasonable to assume that amine-modified ZIFs are also derived by the same way. To verify this assumption, the products ZIF-CoZn3-PhA formed after 5 min, 10 min, 30 min, 1 h, 4 h of reaction were investigated (Figs. S2a–e, S3a in Supporting information). It is found that (1) the nanoparticles (< 10 nm) as shown in Figs. S2a–e prove the self-assembly process; (2) the self-assembly is a fast process which can be completedin 5 min because the precipitation is highly accelerated by the use of external base (amines) [39], which may be also a reason for the smaller ZIF particles; (3) the particle size and structure have no obvious changes over time.

Table 1
The naming rules and correspondence of ZIFs and Co@NCs.

Entry	ZIFs	Co@NCs	Note
1	ZIF-CoZnX-Y[a]	Co@NC-Y-X	/
2	ZIF-Co-PhA	Co@NC-PhA-Co	No use $Zn(NO_3)_2.6H_2O$
3	ZIF-Zn-PhA	NC-PhA	No use $Co(NO_3)_2.6H_2O$
4	ZIF-CoZn3-M[b]	Co@NC-M-3	/
5	ZIF-CoZn3	Co@NC-3	No use of amine

[a] X denotes the mole ratio of $Zn(NO)_3{\cdot}6H_2O/Co(NO)_3{\cdot}6H_2O$ (Zn/Co), Y denotes the type of amine(aniline = PhA, benzylamine = BnA, oleylamine = OA, *n*-butylamine = *n*BuA).

[b] M means the synthesis of ZIFs in MeOH.

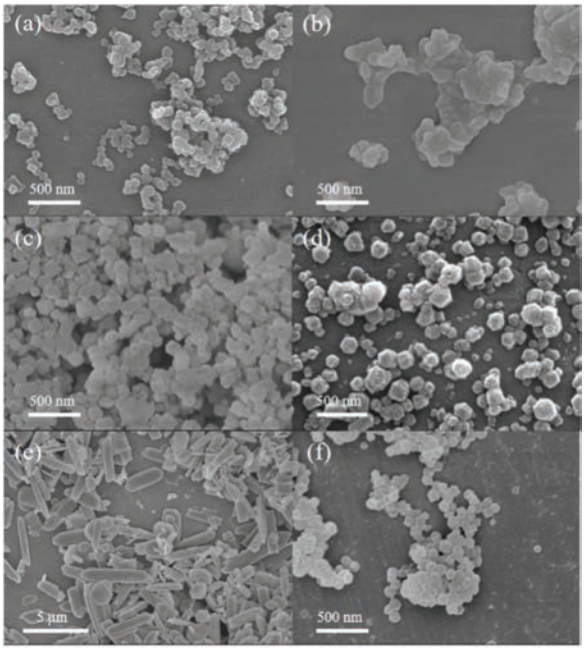

Fig. 1. SEM images of (a) ZIF-CoZn3-PhA, (b) ZIF-CoZn3-OA, (c) ZIF-CoZn3-nBuA, (d) ZIF-CoZn3-BnA, (e) ZIF-CoZn3, (f) ZIF-CoZn3-M.

According to the powder XRD patterns (Fig. S4a in Supporting information), six peaks belonging to the {100}, {11-1}, {2-10}, {200}, {2-11}, {111} planes were detected in the ZIF-CoZn3-M (polyhedron, Fig. 1f) [29]. Additionalpeaks were present in the cases of ZIF-CoZn3 (flat rod, Fig. 1e), ZIF-CoZn3-Y (sphere, Figs. 1a–d). Similarly, six peaks were found in ZIF-CoZn3-Y, but the peak intensity is different from the ZIF-CoZn3-M. Therefore, we demonstrate that amines may change the ratio of crystal faces in ZIFs by coordination with metal ions or absorption on the surface of ZIFs, modifying their size and morphology [35,36,39–41].

As shown in IR spectra, signals of amine (aniline and oleylamine) were observed in both ZIF-CoZn3-PhA and ZIF-CoZn3-OA (Fig. S4b in Supporting information), while benzylamine and *n*-butylamine were removed from corresponding ZIFs owing to their good solubility in water (Fig. S3a). The poor solubility of aniline and oleylamine results more amines absorbed on the surface of ZIFs, which may suppress ZIF particle growth and result in smaller ZIF particles than ZIF-CoZn3-BnA and ZIF-CoZn3-nBuA. Furthermore, the red shift of N—H stretch of aniline (Fig. S4b in Supporting information) suggests the metal ions (Co^{2+} or Zn^{2+}) may coordinate with aniline, which explains why ZIF-CoZn3-PhA has the smallest ZIF particle size.

The topography of amine-modified ZIFs derived Co@NC-Y-3 was also assessed by SEM observation. The morphology of ZIFs can be preserved with partial shrinkage after calcination (Figs. S5a–d in Supporting information). In the cases of Co@NC-3 and Co@NC-M-3 (Figs. S5e and f in Supporting information), the structure of ZIFs is destroyed after sintering. The high treatment temperature (900 °C) is necessary, because it not only promotes the evaporation of Zn, resulting in higher surface areas of Co@NCs, but also facilitates the formation of carbon with high graphitizationthat is beneficial to the electronic interactions in Co@NCs.

After the successful preparation of these Co@NCs, we investigated the catalytic performance of these materials for oxidative esterification of HMF (Fig. 2). It can be concluded that the use of amine type and the molar ratio of Zn/Co in the synthetic process have an obvious influence on the catalytic performance of Co@NCs. Moderate yields of FDMC was achieved at room temperature under

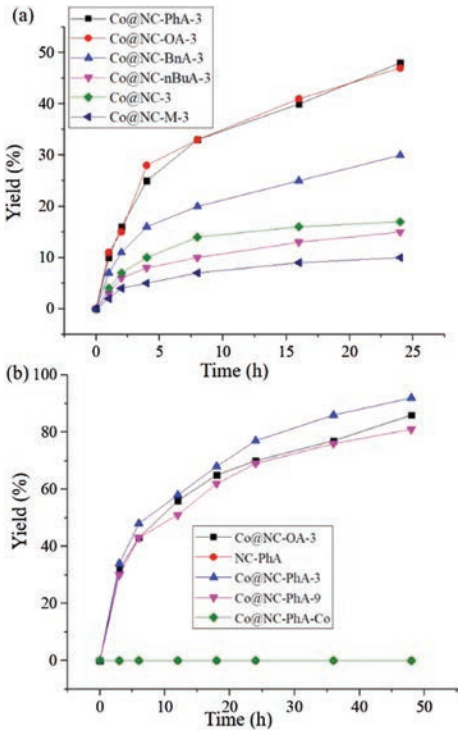

Fig. 2. The effect of preparation process parameters of Co@NCs: (a) amine type and (b) the molar ratio of Zn/Co on catalytic performance for oxidative esterification of HMF. Conditions: HMF 0.3 mmol, Co@NCs (a) 10 mg or (b) 20 mg, MeOH 3 mL, O_2 1 atm, 25 °C, (a) 24 h or (b) 48 h; GC yields with anisole as an internal standard.

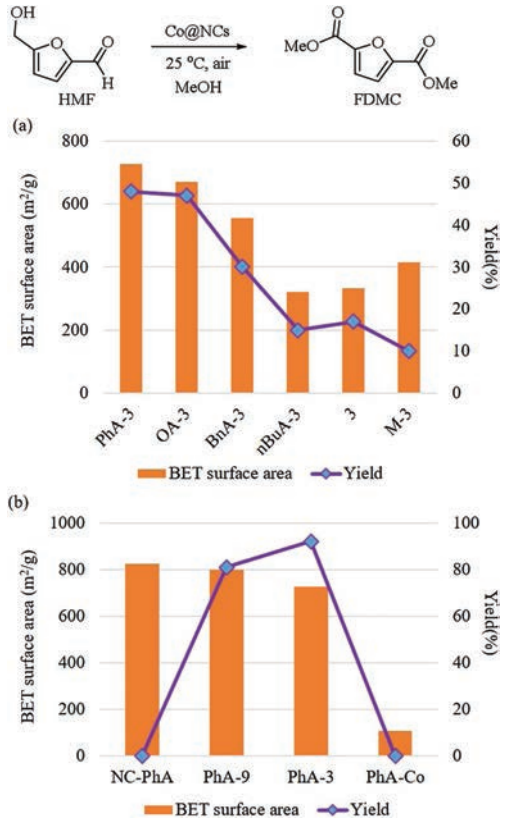

Fig. 3. The relationship between yields (purple points) of FDMC (or BET surfaces areas of Co@NCs (brown square)) with different preparation process parameters of Co@NCs: (a) amine type; (b) molar ratio of Zn/Co. Conditions: HMF 0.3 mmol, Co@NCs (a) 10 mg or (b) 20 mg, MeOH 3 mL, O_2 1 atm, 25 °C, (a) 24 h or (b) 48 h; GC yields with anisole as an internal standard.

air atmosphere (1 atm) when Co@NC-PhA-3 and Co@NC-OA-3 were employed as thecatalysts. Excellent yields of FDMC (92%) could be realized by increasing the amount of catalyst to 20 mg and prolonging the reaction time to 48 h.

Compared with previous works (Table S2), Co@NC-PhA-3 exhibited superior catalytic performance. To the best of our knowledge, this is the first example on the oxidative esterification of HMF under ambient conditions using a non-noble metal catalyst.

Encouraged by the excellent performance of Co@NC-PhA-3, we carried on to investigate the structure-effect relationship between Co@NCs and the reactions.

As shown in Fig. 3, both amine type and molar ratio of Zn/Co have significant influences on the BET surface areas of Co@NCs, which affect the yield of FDMC. With smaller particle size of Co@NCs, the corresponding higher BET surface area can enhance the yield of FDMC owing to the improvement of the interaction between catalyst and reactant (Fig. 3a). Increasing the amount of zinc results in larger BET surface area due to the evaporation of Zn (Fig. 3b), but it also reduces the amount of Co inCo@NCs (Table S3 in Supporting information). Among all specimens, Co@NC-PhA-3 provides the best result.

The TEM images of Co@NCs are shown in Fig. 4. The average Co nanoparticle size of Co@NC-PhA-3 is the smallest than all other Co@NCs (Figs. 4a–e, Table S4 in Supporting information). No obvious Co nanoparticles are found in Co@NC-PhA-9 (Fig. 4f) owing to its low Co content (Table S3).

A carbon shell on Co nanoparticles was observed in the case of Co@NC-PhA-3 (Fig. 4a). It may be derived from the mixture of aniline and 2-methylimidazole. Its presence is conducive to the effective protection of active cobalt nanoparticles from leaching, and inhibitive to the aggregation of cobalt nanoparticles. In the view of BET and TEM results, Co@NC-PhA-Co has low BET surface area (Fig. 3b) and large Co NPs (Fig. 4e), thus it shows no reactivity.

The HRTEM images further verify the existence of the carbon shells (Figs. 5a and b). The clear lattice fringes of 0.205 nm, 0.215 nm and 0.356 nm were observed from the HRTEM image of Co@CN-PhA corresponding to Co (111), Co (100) and graphite respectively (Fig. 5b) [42,43]. The results of TEM-EDS indicate that Co@NC-PhA-3 mainly contains C, O, N, Zn and Co elements, and most of cobalt element is from Co NPs. (Fig. 5c). The residual zinc in the catalyst can increase Lewis basic sites and decrease the strong Lewis acidic sites, which can improve the performance of the catalyst [20].

In order to further check the elemental composition and chemical state, the XRD (Fig. S6 in Supporting information) and XPS results of Co@NCs (Fig. 6) were studied. Characteristic diffraction peaks observed at 44.4°, 51.6°, and 75.9° could be attributed to fcc-structured Co(111), Co(200) and Co(220) planes respectively [43]. The weak diffraction peaks of hcp-structured Co(100) (or Co_2C) and Co(101) correspond to the shifts in 41.5° and 48.4° [44,45]. No obvious diffraction peak of metal is found in the cases of Co@NC-PhA-9 owing to its low Co content. It can also be found that the intensity of Co signal is inversely proportional to the Zn/Co molar ratio. Meanwhile, the structure of Co NPs tends to disorder by increasing the Zn/Co molar ratio.

The XPS also proves that Co@NC-PhA-3 mainly contains C, O, N, Zn and Co elements (Fig. S7 in Supporting information). CoN_x sites exist in the material based on the N 1s region of XPS spectra (Fig. 6b) [23]. Because cobalt phthalocyanine (PcCo) has CoN_4 sites, the single of CoN_x can be further confirmed by comparison of XPS N 1s region of PcCo and Co@NC-PhA-3 (Fig. S8b in Supporting information) [25]. According to XPS results, the N content of Co@NC-PhA-3 is higher than Co@NC-M-3 (Table S5 in Supporting

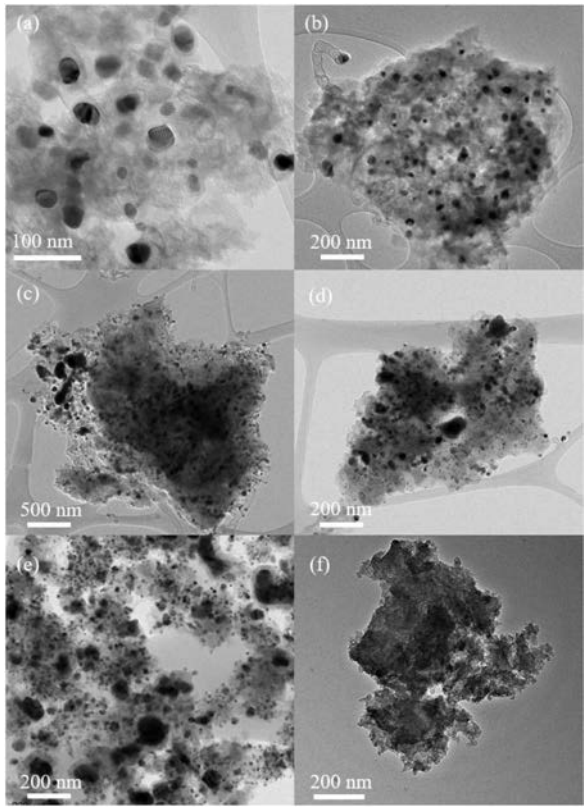

Fig. 4. TEM images of (a) Co@NC-PhA-3, (b) Co@NC-OA-3, (c) Co@NC-3, (d) Co@NC-M-3, (e) Co@NC-PhA-Co, (f) Co@NC-PhA-9.

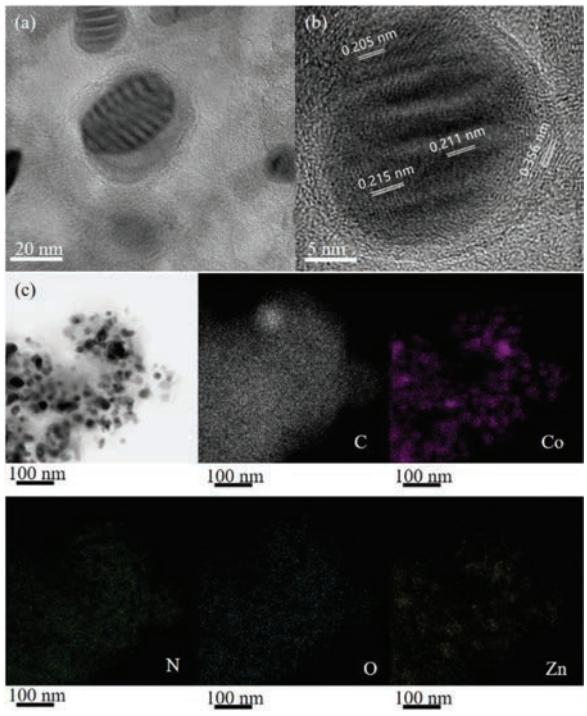

Fig. 5. (a, b) HRTEM images of Co@NC-PhA-3; (c) TEM and its corresponding element mapping images of Co@NC-PhA-3.

information), presumably owing to the presence of aniline in the surface of ZIF-CoZn3-PhA, which is not only an N source but also promote the formation of carbon shell around Co NPs. The high N content can enhance the Co NPs performance by the Mott-Schottky effect for the oxidative esterification of 5-hydroxymethylfurfural [21,22].

To clarify the catalytically active sites of Co@NC-PhA-3 for this reaction, several controlled experiments were carried out (Fig. 7). Firstly, the catalyst was leached with acid (1 mol/L HCl, 120 °C, 12 h) to remove Co NPs, denoted as Co@NC-PhA-3A. The TEM and XRD results suggest that no obviously Co NPs are found in Co@NC-PhA-3A (Fig. S9 in Supporting information). A remarkable decrease in yield of FDMC (19%) was observed using Co@NC-PhA-3A as the catalyst, which suggests Co NPs in Co@NC-PhA-3 are necessary for the reaction. It is well known that SCN^- can poison MN_x sites in catalysis [25,46]. The yield of FDMC was poor (29%) when both Co@NC-PhA-3 and NaSCN (10 mol%) were used, indicating that CoN_x sites can boost the reaction.

Notably, naked Co NPs and Co@AC as the analogs of Co NPs in Co@NC-PhA-3 failed to yield the final product. As shown in Fig. S10 (Supporting information), the naked Co NPs have irregular shape and large size (> 150 nm), and the Co NPs mainly on the surface of AC are easy to aggregate and disappear in the case of Co@AC, which can explain the poor catalytic performance of naked Co NPs and Co@AC. Moreover only trace of FDMC was obtained when PcCo was used as the analog of CoN_x in Co@NC-PhA-3. These results demonstrate the crucial roles of N-doped porous carbon with high graphitization for the reaction, which may promote the absorption and activation of reactants, improve the catalytic performance of Co sites, and enhance the interaction between Co sites and reactants [18–20].

Based on these results, we can safely conclude that there is a synergistic catalytic effect between CoN_x sites and Co NPs in Co@NC-PhA-3 for the reaction. According to the XPS results (Fig. 6a, Fig. S8 and Table S6 in Supporting information), The binding energy of Co^{II} and Co^{III} in Co@NC-PhA-3 shift to a lower value compared with PcCo and Co@NC-M-3, implying Co NPs transfer the electron to CoN_x.

Three simple models CoN_4, Co_6O_2 and CoN_4-Co_6O_2 were established which represent CoN_x, Co NPs and Co@NC-PhA-3 respectively (Fig. 8). The electron number of Co in CoN_4 was calculated from baderde composition of charge density. It is found that adding of Co_6O_2 to CoN_4 can increase the electron number of Co in CoN_4, thus supporting that Co NPs transfer the electron to CoN_x.

To further verify the synergistic catalytic effects of CoN_x sites and Co NPs, the adsorption energies (E_{ads}) of 2-hydroxymethylfurane (FM) and O_2 on different Co sites in all three models are calculated (Fig. 9). Cased on these calculations, we are able to conclude that (1) Both the E_{ads} of O_2 and FM on Co_6O_2 are stronger than CoN_4. (2) Too strong E_{ads} of O_2 on Co_6O_2 may be harmful to the release of active oxygen species, resulting in the oxidation of Co_6O_2. Thus CoN_4 may be the better sites for the activity of O_2 due to its weak E_{ads} of O_2 [25]. (3) The electron transfer from C_6O_2 to CoN_4 can enhance the electron transfer from CoN_4 to O_2 and reduce the E_{ads} of O_2 which are beneficial to the formation and release of active oxygen species [22,47]. (4) The huge difference in E_{ads} of FM between Co_6O_2 and CoN_4 suggests that the absorption of FM mainly takes place on Co_6O_2.

Considering all above results, the tentative synergistic catalysis by CoN_x and Co NPs for α-C-H dissociation of alcohol that is the rate determination step in the oxidative esterification of HMF [18–20], was illustrated in Fig. S11 (Supporting information). Both Co NPs and CoN_x in Co@NC-PhA-3 can activate O_2 while Co NPs bind and oxidize alcohol owing to that the absorption of alcohol mainly takes place on CoNPs. Meanwhile, the electron transfer from Co NPs to CoN_x is beneficial to the formation and release of active oxygen species.

The reusability of Co@NC-PhA-3 was also been studied (Fig. S13a in Supporting information). This material could be

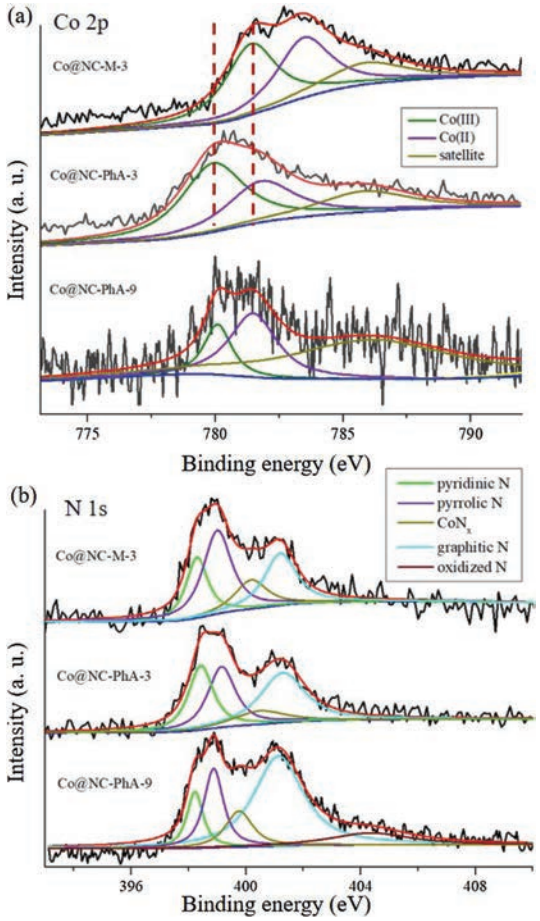

Fig. 6. XPS spectra of (a) Co $2p_{3/2}$ and (b) N 1s of Co@NC-M-3, Co@NC-PhA-3, Co@NC-PhA-9.

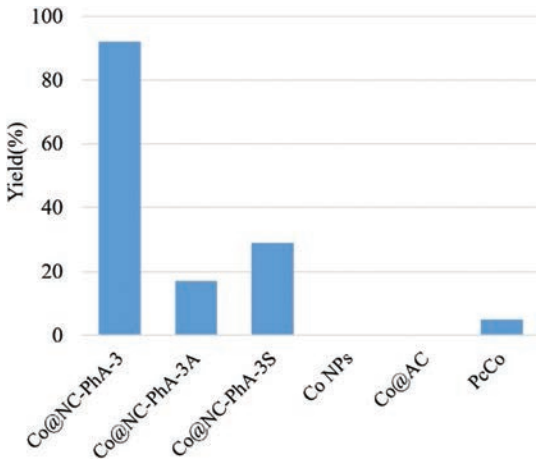

Fig. 7. Comparison of catalytic performance over different catalysts for the oxidative esterification of HMF. Co@NC-PhA-3A means Co@NC-PhA-3 leaching with acid; Co@NC-PhA-3S means the use of Co@NC-PhA-3 with NaSCN (10 mol%); Co@AC meansactive carbon supported Co nanoparticles; PcCo means cobalt phthalocyanine; Co NPs means naked Co nanoparticles.

reused for at least six times without significant loss of catalytic activity. The ICP, TEM, SEM and XPS results of Co@NC-PhA-3 after six cycles (Fig. S12 and Table S3 in Supporting information) suggest that (1) the cobalt leaching was negligible; (2) the shape and size of carbon and cobalt particles were well reserved; (3) no obvious

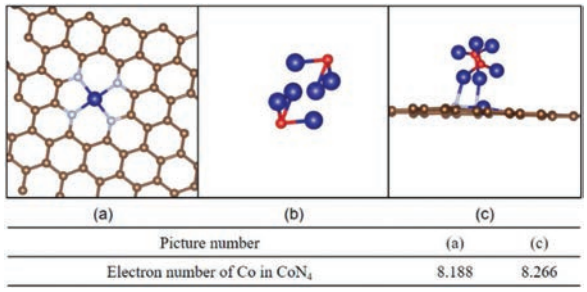

Picture number	(a)	(c)
Electron number of Co in CoN_4	8.188	8.266

Fig. 8. Three calculation models of (a) CoN_4, (b) Co_6O_2 and (c) CoN_4-Co_6O_2 and electron number of Co in CoN_4. Brown is C; red is O; blue is Co; silver is N.

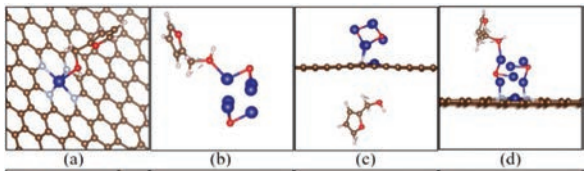

Sites of Co	CoN_4	Co_6O_2	CoN_4 of CoN_4-Co_6O_2	Co_6O_2 of CoN_4-Co_6O_2
E_{ads} of FM (eV)	-0.087	-0.717	-0.068	-0.704
E_{ads} of O_2 (eV)	-0.730	-2.976	-0.471	-3.038

Fig. 9. The adsorption energies of 2-hydroxymethylfurane (FM) and O_2 on different Co sites. FM on (a) CoN_4, (b) Co_6O_2, (c) CoN_4 of CoN_4-Co_6O_2, (d) Co_6O_2 of CoN_4-Co_6O_2; O_2 on (e) CoN_4, (f) Co_6O_2, (g) CoN_4 of CoN_4-Co_6O_2, (h) Co_6O_2 of CoN_4-Co_6O_2. Brown is C; red is O; blue is Co; silver is N.

valence change on the surface of Co in Co@NC-PhA after six cycles wasobserved. The heterogeneous nature of the catalyst was demonstrated by a filtration experiment (Fig. S13b in Supporting information). The catalyst was filtered off after 12 h at room temperature, and the isolated solution was allowed to react for a further 36 h. No further increase in yield was observed.

In summary, we have developed an efficient, sustainable and scalable strategy for the synthesis of porous Co@NCs using aniline-modified ZIFs as the precursor. Aniline can coordinate and absorb on the surface of ZIFs, and accelerate the precipitation of ZIFs, by which smaller particle size of ZIF (ZIF-CoZn3-PhA) are obtained. Notably, several excellent properties of Co@NC-PhA-3 including higher specific surface area, the protective carbon shell of smaller Co NPs and higher the nitrogen content. These are attributed to aniline on the surface of ZIF-CoZn3-PhA, and can enhance the performance of the catalyst. Co@NC-PhA-3 exhibits promising performance and recyclability for base-free oxidative esterification of HMF. Based on our characterization, experiments and calculations, a synergistic catalytic effect between CoN_x sites and Co NPs has been disclosed. Both Co NPs and CoN_x activate O_2 while Co NPs bind and oxidize HMF. Meanwhile, the electron transfer from Co NPs to CoN_x is beneficial to the formation and release of active oxygen species.

Declaration of competing interest

The authors declare that they have no known competing financial interests or personal relationships that could have appeared to influence the work reported in this paper.

Acknowledgments

We gratefully acknowledge the Fundamental Research Funds for the Central Universities (No. 30920021120) and Key Laboratory of Biomass Energy and Material, Jiangsu Province (No. JSBEM201912) for financial support. This work was a project funded by the Priority Academic Program development of Jiangsu Higher Education Institution. We also thank Analysis and Test Center Nanjing University & Technology for the help in obtaining the IR and XRD date.

Appendix A. Supplementary data

Supplementary material related to this article can be found, in the online version, at doi:https://doi.org/10.1016/j.cclet.2020.06.027.

References

[1] Y. Romn-Leshkov, C.J. Barrett, Z.Y. Liu, Nature 447 (2007) 982–986.
[2] C. Liu, M. Wei, J. Wang, J. Xu, J. Jiang, K. Wang, ACS Sustain. Chem. Eng. 8 (2020) 5776–5786.
[3] X. Kong, Y. Zhu, Z. Fang, et al., Green Chem. 20 (2018) 3657–3682.
[4] Z. Zhang, K. Deng, ACS Catal. 5 (2015) 6529–6544.
[5] F.A. Kucherov, E.G. Gordeev, A.S. Kashin, V.P. Ananikov, Angew. Chem. Int. Ed. 56 (2017) 15931–15935.
[6] I. Delidovich, P.J. Hausoul, L. Deng, et al., Chem. Rev. 116 (2016) 1540–1599.
[7] C.F. Araujo, M.M. Nolasco, P.J.A. Ribeiro-Claro, et al., Macromolecules 51 (2018) 3515–3526.
[8] E. Taarning, I.S. Nielsen, K. Egeblad, R. Madsen, C.H. Christensen, ChemSusChem 1 (2008) 75–78.
[9] O. Casanova, S. Iborra, A. Corma, J. Catal. 265 (2009) 109–116.
[10] F. Menegazzo, T. Fantinel, M. Signoretto, F. Pinna, M. Manzoli, J. Catal. 319 (2014) 61–70.
[11] F. Menegazzo, M. Signoretto, D. Marchese, F. Pinna, M. Manzoli, J. Catal. 326 (2015) 1–8.
[12] J. Deng, H.J. Song, M.S. Cui, Y.P. Du, Y. Fu, ChemSusChem 7 (2014) 3334–3340.
[13] Y. Sun, H. Ma, X. Jia, et al., ChemCatChem 8 (2016) 2907–2911.
[14] X. Tong, L. Yu, H. Chen, et al., Catal. Commun. 90 (2017) 91–94.
[15] A. Cho, S. Byun, J.H. Cho, B.M. Kim, ChemSusChem 12 (2019) 2310–2317.
[16] F. Li, X.L. Li, C. Li, J. Shi, Y. Fu, Green Chem. 20 (2018) 3050–3058.
[17] A. Salazar, P. Hunemorder, J. Rabeah, et al., ACS Sustain. Chem. Eng. 7 (2019) 12061–12068.
[18] H. Zhou, S. Hong, H. Zhang, et al., Appl.Catal. B: Environ. 256 (2019) 117767.
[19] K.K. Sun, S.J. Chen, Z.L. Li, G.P. Lu, C. Cai, Green Chem. 21 (2019) 1602–1608.
[20] Y. Lin, G.P. Lu, X. Zhao, et al., Mole. Catal. 482 (2020) 110695.
[21] H. Su, K.X. Zhang, B. Zhang, et al., J. Am. Chem. Soc. 139 (2017) 811–818.
[22] Y. Feng, W. Jia, G. Yan, et al., J. Catal. 381 (2020) 570–578.
[23] D. Eisenberg, T.K. Slot, G. Rothenberg, ACS Catal. 8 (2018) 8618–8629.
[24] T.K. Slot, D. Eisenberg, G. Rothenberg, ChemCatChem 10 (2018) 2119–2124.
[25] W.J. Jiang, L. Gu, L. Li, et al., J. Am. Chem. Soc. 138 (2016) 3570–3578.
[26] G. Zhong, D. Liu, J. Zhang, J. Mater. Chem. A 6 (2018) 1887–1899.
[27] Y.Z. Chen, C. Wang, Z.Y. Wu, et al., Adv. Mater. 27 (2015) 5010–5016.
[28] K.K. Sun, S. Chen, J. Zhang, G.P. Lu, C. Cai, ChemCatChem 11 (2019) 1264–1271.
[29] D.W. Lewis, A.R. Ruiz-Salvador, A. Gómez, et al., CrystEngComm 11 (2009) 2272–2276.
[30] D. Yu, L. Ge, B. Wu, et al., J. Mater. Chem. A 3 (2015) 16688–16694.
[31] Q. Liao, M. He, Y. Zhou, et al., ACS Appl. Mater. Inter. 10 (2018) 29136–29144.
[32] G. Fang, J. Zhou, C. Liang, et al., Nano Energy 26 (2016) 57–65.
[33] Y. Pan, Y. Liu, G. Zeng, L. Zhao, Z. Lai, Chem. Commun. 47 (2011) 2071–2073.
[34] Y. Deng, Y. Dong, G. Wang, et al., ACS Appl. Mater. Inter. 11 (2017) 9699–9709.
[35] K. Liang, R. Ricco, C.M. Doherty, M.J. Styles, P. Falcaro, CrystEngComm 18 (2016) 4264–4267.
[36] Y. Pan, D. Heryadi, F. Zhou, et al., CrystEngComm 13 (2011) 6937.
[37] K.K. Sun, J.L. Sun, G.P. Lu, C. Cai, Green Chem. 21 (2019) 4334–4340.
[38] J. Zhang, T. Zhang, D. Yu, K. Xiao, Y. Hong, CrystEngComm 17 (2015) 8212–8215.
[39] C. Avci, J. Ariñez-Soriano, A. Carné-Sánchez, et al., Angew. Chem. Int. Ed. 54 (2015) 14417–14421.
[40] T. Tsuruoka, S. Furukawa, Y. Takashima, et al., Angew. Chem. 48 (2009) 4739–4743.
[41] N. Stock, S. Biswas, Chem. Rev. 112 (2012) 933–969.
[42] B. Liu, L. Jin, H. Zheng, et al., ACS Appl. Mater. Inter. 9 (2017) 1746–1758.
[43] V.L. Kuznetsov, I.L. Zilberberg, Y.V. Butenko, A.L. Chuvilin, B. Segall, J. Appl. Phys. 86 (1999) 863–870.
[44] J.C. Wang, R.F. Nie, L. Xu, X.L. Lyu, X.Y. Lu, Green Chem. 21 (2019) 314–320.
[45] Z. Zhao, W. Lu, R. Yang, et al., ACS Catal. 8 (2018) 228–241.
[46] Z. Ma, T. Song, Y. Yuan, Y. Yang, Chem. Sci. 10 (2019) 10283–10289.
[47] Q. Gu, P. Sautet, C. Michel, ACS Catal. 8 (2018) 11716–11721.